THE JOURNAL OF BIOLOGICAL CHEMISTRY VOL. 283, NO. 12, pp. 7455–7463, March 21, 2008
© 2008 by The American Society for Biochemistry and Molecular Biology, Inc. Printed in the U.S.A.

Preferential Assembly of Epithelial Sodium Channel (ENaC) Subunits in *Xenopus* Oocytes

ROLE OF FURIN-MEDIATED ENDOGENOUS PROTEOLYSIS[*]

Received for publication, September 4, 2007, and in revised form, January 10, 2008 Published, JBC Papers in Press, January 14, 2008, DOI 10.1074/jbc.M707399200

Michael Harris[‡], **Agustin Garcia-Caballero**[§], **M. Jackson Stutts**[§], **Dmitri Firsov**[‡], **and Bernard C. Rossier**[‡1]

From the [‡]*Département de Pharmacologie et Toxicologie, Université de Lausanne, CH-1005 Lausanne, Switzerland and the* [§]*Cystic Fibrosis/Pulmonary Research and Treatment Center, University of North Carolina, Chapel Hill, North Carolina 27599*

The epithelial sodium channel (ENaC) is preferentially assembled into heteromeric $\alpha\beta\gamma$ complexes. The α and γ (not β) subunits undergo proteolytic cleavage by endogenous furin-like activity correlating with increased ENaC function. We identified full-length subunits and their fragments at the cell surface, as well as in the intracellular pool, for all homo- and heteromeric combinations (α, β, γ, $\alpha\beta$, $\alpha\gamma$, $\beta\gamma$, and $\alpha\beta\gamma$). We assayed corresponding channel function as amiloride-sensitive sodium transport (I_{Na}). We varied furin-mediated proteolysis by mutating the P1 site in α and/or γ subunit furin consensus cleavage sites (α_{mut} and γ_{mut}). Our findings were as follows. (i) The β subunit alone is not transported to the cell surface nor cleaved upon assembly with the α and/or γ subunits. (ii) The α subunit alone (or in combination with β and/or γ) is efficiently transported to the cell surface; a surface-expressed 65-kDa α ENaC fragment is undetected in $\alpha_{mut}\beta\gamma$, and I_{Na} is decreased by 60%. (iii) The γ subunit alone does not appear at the cell surface; γ co-expressed with α reaches the surface but is not detectably cleaved; and γ in $\alpha\beta\gamma$ complexes appears mainly as a 76-kDa species in the surface pool. Although basal I_{Na} of $\alpha\beta\gamma_{mut}$ was similar to $\alpha\beta\gamma$, γ_{mut} was not detectably cleaved at the cell surface. Thus, furin-mediated cleavage is not essential for participation of α and γ in $\alpha\beta\gamma$ heteromers. Basal I_{Na} is reduced by preventing furin-mediated cleavage of the α, but not γ, subunits. Residual current in the absence of furin-mediated proteolysis may be due to non-furin endogenous proteases.

The highly sodium-selective epithelial sodium channel (ENaC)[2] is composed of three homologous subunits (α, β, and γ) and is expressed in several ion-transporting epithelia, including the kidney, colon, and lung (1). The membrane topology of each subunit was predicted to consist of two transmembrane domains with short cytoplasmic amino and carboxyl termini and joined by a large extracellular loop. This prediction is strongly supported by recent crystallization of ENaC relative ASIC1. The ASIC1 structure (2) also makes it clear that ENaC is likely a heterotrimer ($\alpha_1\beta_1\gamma_1$), in contrast to the heterotetrameric, octameric, or nonameric stoichiometry ($\alpha\beta\alpha\gamma$) proposed previously (3–5). In the *Xenopus* oocyte expression system, it has been possible to quantitate the number of channel complexes expressed at the cell surface and to measure in the same oocyte the amiloride-sensitive current generated by the expression of ENaC at the membrane (6, 7). This assay demonstrated the preferential assembly of $\alpha\beta\gamma$ channels. Maximal ENaC activity measured by the amiloride-sensitive inward current (I_{Na}) is observed only when the α, β, or γ subunits are co-injected in the *Xenopus* oocyte expression system. There is an excellent correlation between I_{Na} and the number of channel complexes expressed at the cell surface (7). When the α subunit is injected alone (presumably $\alpha3$ trimers), only 1 or 2% of maximal activity is observed. When the α/β or α/γ subunits are co-injected (potentially forming $\alpha_2\beta_1$, $\alpha_1\beta_2$, $\alpha_2\gamma_1$, or $\alpha_1\gamma_2$), 5–15% of maximal activity is recorded. The β or γ subunit alone does not lead to any significant channel activity, whereas expression of the β/γ subunits leads to very small activity (2%) after prolonged incubation (6–7 days after injection) (8). These data indicated that the α subunit has an essential chaperone role, bringing the β and γ subunits to the plasma membrane, but the β and γ subunits are also essential for optimal expression of channel complexes at the cell surface.

The endogenous processing of ENaC in heterologous expression systems is significant and specific for each subunit. Hughey *et al.* (9) showed that when tagged subunits were expressed alone in Chinese hamster ovary or Madin-Darby canine kidney type 1 epithelia, the α (95 kDa), β (96 kDa), and γ (93 kDa) subunits each produced a single band on SDS gels by immunoblotting. However, co-expression of the $\alpha\beta\gamma$ ENaC subunits revealed a second band for each subunit (65 kDa for α, 110 kDa for β, and 75 kDa for γ). The smaller size of the processed α and γ subunits was consistent with proteolytic cleavage. Hughey *et al.* (10) have subsequently implicated furin in ENaC proteolytic processing. They demonstrated that the α and γ ENaC subunits may be cleaved during maturation at consensus sites for furin cleavage. Using site-specific mutagenesis of the key P1 arginine in the R*XX*R(P1) furin sequences in α and γ, ENaC expression in furin-deficient cells, and furin-specific inhibitors, the authors proposed that ENaC cleavage correlated with channel

* This work was supported by a 2003 grant from the Novartis Foundation (to B. C. R.), Swiss National Foundation Grants 3100-061966 (to B. C. R.) and 3100A0-105592 (to D. F.), and National Institutes of Health Grant HL034322 (to M. J. S.). The costs of publication of this article were defrayed in part by the payment of page charges. This article must therefore be hereby marked "*advertisement*" in accordance with 18 U.S.C. Section 1734 solely to indicate this fact.

[1] To whom correspondence should be addressed: Dept. de Pharmacologie et Toxicologie, Université de Lausanne, 27 rue du Bugnon, CH-1005 Lausanne, Switzerland. Tel.: 4121-692-5351; Fax: 4121-692-5355; E-mail: Bernard.Rossier@unil.ch.

[2] The abbreviations used are: ENaC, epithelial sodium channel; rENaC, rat ENaC; I_{Na}, amiloride-sensitive inward current; MBS, modified Barth solution; WT, wild type.

activity (10). A demonstration of a direct correlation between endogenous proteolytic cleavage of surface-expressed ENaC and activation in the same expression system was not provided. Important questions remain. Does the processing occur on the exocytic and/or endocytic pathway or at the plasma membrane? What is the relative importance of α *versus* γ cleavage for channel activation? We recently designed an experimental protocol that allows labeling of cell surface-expressed protein (11) and direct correlation of channel cleavage and amiloride-sensitive ENaC-mediated sodium transport (12). However, because both the α and γ subunits undergo endogenous proteolysis, leading to a specific pattern for each subunit expressed at the cell surface, it is not clear whether α and/or γ processing was required for channel activity under base-line conditions. We reasoned that if cleavage of the α and/or γ ENaC subunits takes place at the plasma membrane, causing channel activation, there should be a precursor-product relationship between the pool of full-length uncleaved channel (precursor associated with little or no ENaC activity) and the pool of cleaved channel (product associated with increased ENaC activity). We co-injected the α, β, and γ subunits in all combinations and measured I_{Na} and the size of channel subunits expressed at the cell surface (biotinylated proteins) or in the intracellular pool (non-biotinylated proteins) to establish a direct correlation between cell surface expression of cleaved subunit and sodium transport. Using the α and/or γ ENaC subunits with furin cleavage site mutations, we provide evidence that ENaC activation during preferential assembly requires furin-dependent and furin-independent processing.

EXPERIMENTAL PROCEDURES

cRNAs—Complementary RNAs of rat $\alpha\beta\gamma$ ENaC subunits were synthesized *in vitro* using SP6 and T7 RNA polymerase. C terminally V5 epitope-tagged α, β, and γ ENaC subunits were created by PCR amplification. For each subunit, two primers were synthesized. The forward primer contains the SpeI site and the start codon of the ENaC gene; the reverse primer contains the I site, the coding sequence for V5, and the C-terminal sequence of the ENaC gene. PCR products were purified and cloned into the SpeI/NotI sites of vector pSDE. Furin mutants were engineered as described by Hughey *et al.* (10) using C terminally V5 epitope-tagged α or γ subunits. In the present study we used the αR205A/R231A mutant (α_{mut}) and γR138A (γ_{mut}).

Antibodies—Monoclonal anti-V5 antibody was obtained from Invitrogen and used according to the manufacturer's instructions. The actin antibody was from Sigma.

Expression of ENaC cRNA in Xenopus Oocytes—The cRNAs were injected into *Xenopus* oocytes (3.3 ng of each subunit) and kept in modified Barth solution (MBS) containing 88 mM NaCl, 1 mM KCl, 2.4 mM $NaHCO_3$, 0.8 mM $MgSO_4$, 0.3 mM $Ca(NO_3)_2$, 0.4 mM $CaCl_2$, and 10 mM Hepes-NaOH (pH 7.2). Electrophysiological measurements and cell surface biotinylation were performed 24 h after injection. I_{Na} was recorded using a two-electrode voltage clamp and was defined as the difference between Na^+ currents obtained in the presence and absence of amiloride (5 μM).

Biotinylation of ENaC Subunits on the Cell Surface—Biotinylation was performed in 40-well plates using 50 oocytes/experimental condition as described (11, 12). All biotinylation steps were performed at 4 °C. After incubation in MBS for 30 min at 4 °C, the oocytes were washed three times with MBS. After the last wash, the MBS was removed and replaced by a biotinylation buffer containing 10 mM triethanolamine, 150 mM NaCl, 2 mM $CaCl_2$, and 1 mg/ml EZ-Link Sulfo-NHS-SS-Biotin (Pierce) (pH 9.5). The incubation lasted 15 min with gentle agitation. The biotinylation reaction was stopped by washing the oocytes two times with quench buffer containing 192 mM glycine and 25 mM Tris-Cl (pH 7.5) added to MBS. After the second wash, oocytes were incubated for 5 min in the quench buffer with gentle agitation. Oocytes were then washed two times with MBS and lysed by repeated pipetting with Pasteur pipettes in lysis buffer containing 1% Triton X-100, 500 mM NaCl, 5 mM EDTA, 50 mM Tris-Cl, and 5 mg/ml each leupeptin, antipain, and pepstatin (20 μl/oocyte). The lysates were vortexed for 30 s and centrifuged for 10 min at ~5,000 $\times$ *g*. Supernatants were transferred to new 1.5-ml Eppendorf tubes containing 50 μl of Immuno-Pure-immobilized streptavidin beads (Pierce) washed with lysis buffer. After overnight incubation at 4 °C with agitation, the tubes were centrifuged for 1 min at ~5,000 $\times$ *g*. The supernatant (non-biotinylated pool) was removed, and the beads were washed three times with lysis buffer. 35 μl of 2$\times$ SDS-PAGE sample buffer was added to the beads. All samples were heated for 5 min at 95 °C before being loaded on 8–15% SDS-polyacrylamide gel. Cell surface labeling was restricted to plasma membrane proteins, as shown by the absence of any significant amount of actin in this fraction. Essentially, the non-biotinylated protein pool represents proteins expressed intracellularly (*i.e.* the intracellular pool of membrane- and non-membrane-associated proteins) and is characterized by a large amount of actin. In some experiments, the non-biotinylated protein pool was spun down at 20,000 $\times$ *g* for 20 min to get a crude post-cytoplasmic membrane fraction (the non-biotinylated membrane-enriched pool).

Statistical Analysis—All data are represented as means, and error bars indicate S.E. Statistical significance was determined by analysis of variance and was followed by Bonferroni's post-test when appropriate. A p value <0.05 was considered statistically significant. The number of independent experimental repetitions is represented by n.

RESULTS

α *Subunit*—After a 24-h incubation (Fig. 1*A*), a subunit alone (*lane 1*) did not generate a significant amiloride-sensitive current. Co-expression of α with β (Fig. 1*A*, *lane 2*) or γ (*lane 3*) increased I_{Na} with respect to α-injected (*lane 1*) or non-injected (*lane 13*) oocytes, representing ~15% of maximal activity observed when the $\alpha\beta\gamma$ subunits were co-injected (*lane 4*). A full-length uncleaved 95-kDa α subunit band was predominantly observed at the cell surface (Fig. 1*B*) of α (*lane 1*)-, $\alpha\beta$ (*lane 2*)-, $\alpha\gamma$ (*lane 3*)-, and $\alpha\beta\gamma$ (*lane 4*)-injected oocytes. The predominant cleavage product was a 65-kDa band, although other bands (80 kDa and smaller) were observed but in small and variable proportions upon long film exposure (data not shown). In the non-biotinylated protein pool (Fig. 1*C*), the

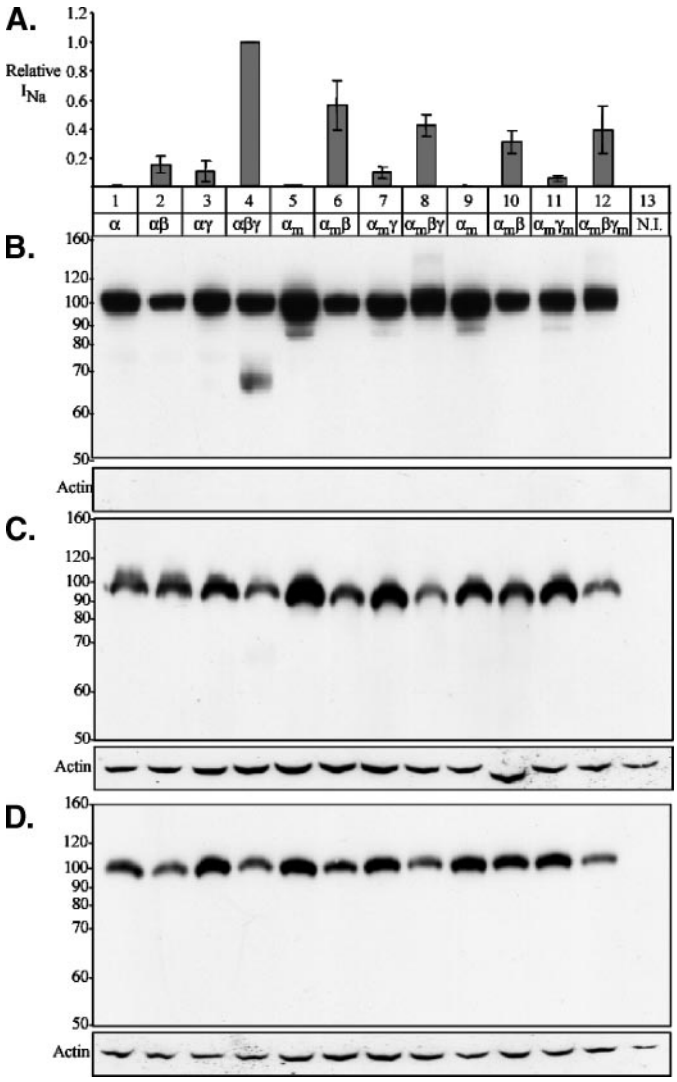

FIGURE 1. **Activity and expression of α rENaC assembled with β rENaC and/or γ rENaC with and without mutations in the α and γ subunit furin cleavage sites.** *Xenopus* oocytes were injected with α, $\alpha\beta$, $\alpha\gamma$, or $\alpha\beta\gamma$ rENaC cRNAs with and without mutations in the furin consensus sites in the α and γ subunits 24 h before experimental analysis. The α rENaC subunit was V5-tagged at the C terminus. Cell surface-biotinylated proteins, non-biotinylated proteins, and membrane-enriched protein fractions were probed with V5 antibody to detect the V5 tag inserted in the C terminus of α ENaC. A representative gel of three experiments (*lanes 1–12*) is shown. Quantitation of the data are shown in Fig. 2. *A*, amiloride-sensitive current. Current was measured by voltage clamp in each experimental condition and expressed relative to current in $\alpha\beta\gamma$ rENaC-injected oocytes (1168 $\pm$ 228 nA; $n = 6$ independent experiments for WT (*lanes 1–4*), $n = 3$ for experiments with α furin site mutations α_{mut} ΔR205A and ΔR231A (*lanes 5–8*), and $n = 3$ for experiments with α furin site and γ furin site mutation γ_{mut} ΔR138A (*lanes 9–12*)). Oocytes injected with $\alpha\beta$ and $\alpha\beta\gamma$ rENaC had a significantly higher amiloride-sensitive current than α and $\alpha\gamma$ rENaC-injected oocytes ($p < 0.05$ and 0.001, respectively). Oocytes injected with $\alpha_{mut}\beta$ rENaC and $\alpha_{mut}\beta\gamma$ rENaC had a significantly higher amiloride-sensitive current than α and $\alpha\gamma$ rENaC-injected oocytes ($p < 0.05$ and 0.001, respectively). Interestingly, $\alpha_{mut}\beta$ rENaC-injected oocytes had significantly more current than $\alpha\beta$ rENaC-injected oocytes ($p < 0.05$) and did not differ significantly from $\alpha_{mut}\beta\gamma$ rENaC-injected oocytes. Oocytes injected with $\alpha_{mut}\beta\gamma_{mut}$ rENaC had a significantly higher amiloride-sensitive current than α_{mut}- and $\alpha_{mut}\gamma_{mut}$-injected, but not $\alpha_{mut}\beta$ rENaC-injected, oocytes ($p < 0.001$). *B*, biotinylated cell surface proteins. Full-length 95-kDa α ENaC was detected at the cell surface in all conditions where α rENaC was injected. The 65-kDa α ENaC cleavage product was detected in some but not all experiments; it was present when $\alpha\beta\gamma$ rENaC was injected into the same oocyte but never when oocytes were injected with α_{mut}. *C*, non-biotinylated protein pool. The non-biotinylated protein pool contained full-length 95-kDa α ENaC, but not the 65-kDa cleavage product, in each experimental condition. 95-kDa band was predominantly observed (*lanes 1–4*). Membrane enrichment of the non-biotinylated protein pool revealed the α subunits to be in the full-length 95-kDa form (Fig. 1*D*, *lanes 1–4*).

α_{mut} Subunit—The 65-kDa fragment has been observed *in vivo* and *in vitro* and proposed to be due to furin-mediated proteolysis. To test the possible physiological role of the expression of the putative furin 65-kDa fragment at the cell surface, we directly compared the effect of α_{mut} on I_{Na} and on the pattern of a cleaved α fragment at the cell surface. After 24 h of incubation, the α_{mut} subunit alone (Fig. 1, *B–D*, *lane 5*) did not generate a significant amiloride-sensitive current. Co-expression of α_{mut} with β (*lane 6*) or γ (*lane 7*) increased I_{Na} with respect to non-injected oocytes (*lane 13*) at levels significantly higher ($p < 0.05$) than that observed in WT $\alpha\beta$ (*lane 2 versus lane 6*) and equal to that in $\alpha\gamma$ complexes (*lane 3 versus lane 7*). Co-expression of α_{mut} with β and γ (*lane 8*) resulted in a 60% reduction ($p < 0.01$) in I_{Na}. Co-expression of α_{mut} with β and γ_{mut} (*lane 12*) resulted in a similar 60% reduction ($p < 0.05$) in I_{Na}. Mutation of the furin cleavage sites in the α subunit eliminated the appearance of the 65-kDa cleavage product at the cell surface (Fig. 1*B*, *lanes 5–12*).

Quantitation of six independent α assembly experiments is shown in Fig. 2. Upon preferential assembly of $\alpha\beta\gamma$ complexes, there was no significant change in the biotinylated pool, non-biotinylated protein pool, or membrane-enriched protein pool of the full-length 95-kDa α subunit (Fig. 2, *A–C*, *lanes 1–4*), but there was a small but insignificant increase in the amount of cleaved 65-kDa fragments in the biotinylated pool (*panels A–C*, *lanes 5–8*). There was no detectable 65-kDa band in the non-biotinylated pool or in the membrane-enriched protein pool (Fig. 2, *B* and *C*, *lanes 1–8*). The non-biotinylated membrane-enriched pool showed a progressive but non-significant decrease in the full-length α subunit (Fig. 2*C*, *lanes 1–4*).

Mutation of the furin cleavage sites in the α subunit alone did not change the quantity of the 95-kDa bands in the biotinylated protein pool (Fig. 2*A*, *lanes 9–12*), the non-biotinylated pool (*panel B*, *lanes 9–12*), or the non-biotinylated membrane-enriched pool (*panel C*, *lanes 9–12*). This mutation also eliminated the 65-kDa band in the biotinylated protein pool (Fig. 2*A*, *lanes 13–16*), the non-biotinylated pool (*panel B*, *lanes 13–16*), and the non-biotinylated membrane-enriched pool (*panel C*, *lanes 13–16*).

α_{mut} and γ_{mut} Subunits—Mutation of the furin sites in both the α and γ subunits decreased the amount of 95-kDa bands in $\alpha_{mut}\gamma_{mut}$- and $\alpha_{mut}\beta\gamma_{mut}$-injected oocytes in the biotinylated pool ($p < 0.01$ and 0.001, respectively; Fig. 2*A*, *lanes 19* and *20*), the $\alpha_{mut}\beta\gamma_{mut}$-injected oocytes in the non-biotinylated pool ($p < 0.05$; *panel B*, *lane 20*), and the $\alpha_{mut}\beta\gamma_{mut}$-injected oocytes in the non-biotinylated membrane-enriched pool ($p < 0.001$; *panel C*, *lane 20*). The 65-kDa band was also eliminated in the biotinylated protein pool (Fig. 2*A*, *lanes 21–24*), the non-bio-

D, membrane-enriched proteins. Membrane-enriched protein pellets contained full-length 95-kDa α ENaC, but not the 65-kDa cleavage product, in each experimental condition. Absence of actin in the biotinylated proteins indicated that no intracellular proteins were labeled. Even quantities of actin in the non-biotinylated and membrane-enriched proteins indicated even protein loading. *N.I.*, non-injected oocytes.

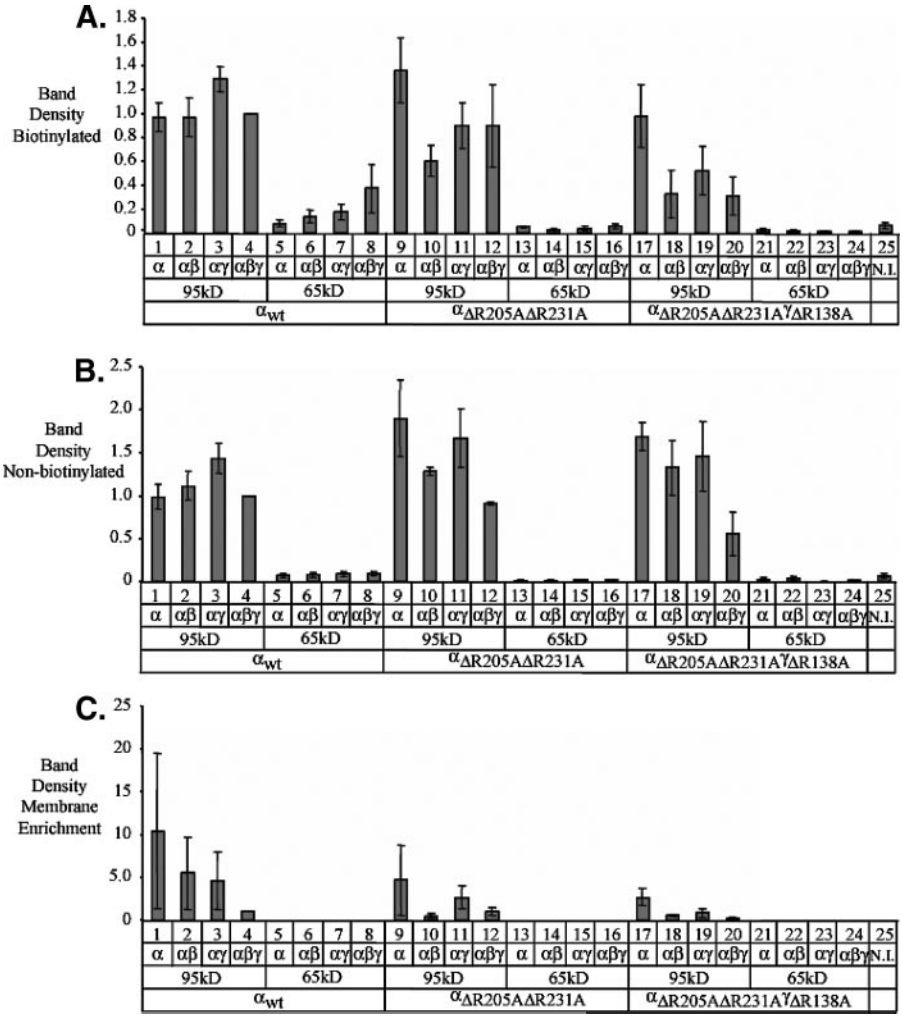

FIGURE 2. **Densitometry of α rENaC cell surface expression when assembled with β rENaC and/or γ rENaC with and without mutations in the α and γ subunit furin cleavage sites.** Western blots of biotinylated, non-biotinylated, and membrane-enriched proteins from *Xenopus* oocytes injected with V5-tagged α rENaC alone and with β rENaC and/or γ rENaC with and without mutations in the α and γ subunit furin cleavage sites were subjected to densitometric analysis. In biotinylated and non-biotinylated experiments, $n = 6$ independent experiments for WT, $n = 3$ for experiments with α furin site mutations α_{mut} ΔR205A and ΔR231A, and $n = 3$ for experiments with α furin site and γ furin site mutation γ_{mut} ΔR138A. In membrane-enriched experiments, $n = 3$ for all conditions. *A*, cell surface biotinylation. No significant difference in band density was detected in the experimental groups in the 95- or 65-kDa bands at the cell surface in wild type- or α_{mut}-injected oocytes. There were significantly fewer 95-kDa bands at the cell surface in $\alpha_{mut}\gamma_{mut}$- and $\alpha_{mut}\beta\gamma_{mut}$-injected oocytes relative to the wild type controls ($p < 0.01$ and 0.001, respectively). *B*, non-biotinylated protein pool. No significant difference in band density was detected in the experimental groups in the 95- or 65-kDa bands in the cell in the wild type- or α_{mut}-injected oocytes, with the exception of the $\alpha_{mut}\beta\gamma$-injected oocytes, which had slightly fewer 95-kDa bands than in wild type $\alpha\beta\gamma$ controls ($p < 0.05$). There were slightly fewer 95-kDa bands in $\alpha_{mut}\beta\gamma$ than in the wild type controls ($p < 0.05$). *C*, membrane-enriched proteins. No significant difference in band density was detected in the experimental groups in the 95- or 65-kDa bands in the cell in wild type- or α_{mut}-injected oocytes. There were significantly fewer 95-kDa bands in the $\alpha_{mut}\beta\gamma_{mut}$-injected than in the wild type-injected oocytes ($p < 0.001$). *N.I.*, non-injected oocytes.

tinylated pool (*panel B*, *lanes 21–24*), and the non-biotinylated membrane-enriched pool (*panel C*, *lanes 21–24*). Collectively, the data indicate that the furin consensus site on the α subunit is required for ENaC activation upon assembly into $\alpha\beta\gamma$ complexes, but 40% of I_{Na} is not accounted for by this mechanism. Interestingly, the activation observed when α is assembled into the $\alpha\beta$ heterodimer is not inhibited but rather enhanced, suggesting that the β subunit may also play a distinct furin-independent role in ENaC activation.

β Subunit—After a 24-h incubation (Fig. 3*A*), the β subunit alone (*lane 1*) or $\beta\gamma$ subunits together (*lane 3*) did not generate a significant current, whereas $\alpha\beta$ (*lane 2*) or $\alpha\beta\gamma$ (*lane 4*) significantly increased I_{Na} with respect to β-injected (*lane 1*) or non-injected (*lane 5*) oocytes. At the cell surface (Fig. 3*B*), a single molecular mass species (105 kDa) of the β subunit was detected in $\alpha\beta\gamma$-injected oocytes (*lane 4*) and in small proportions in $\alpha\beta$-injected oocytes with no evidence of cleavage or processing. In the non-biotinylated protein pool (Fig. 3*C*), a single molecular mass species (105 kDa) of the β subunit was detected in all conditions (*lanes 1–4*) with no evidence of cleavage or processing. We conclude that the β subunit cannot traffic to the plasma membrane unless accompanied by the α subunit. Quantitation is shown in Fig. 4. The amount of β subunits detected at the cell surface in β-, $\alpha\beta$-, or $\beta\gamma$-injected oocytes was small and not significantly different from background (non-injected oocytes), whereas the amount of β subunits detected in $\alpha\beta\gamma$-injected oocytes was significant compared with controls. There were no significant differences in the amount of β subunits detected in the non-biotinylated protein (intracellular) pool.

γ Subunit—After a 24-h incubation (Fig. 5*A*), the γ subunit expressed alone (*lane 1*) or in $\beta\gamma$-injected oocytes (*lane 3*) did not generate any significant amiloride-sensitive current, whereas γ co-expressed with α (*lane 2*) yielded ~5% of maximal activity observed when the $\alpha\beta\gamma$ subunits were co-injected (*lane 4*). At the cell surface (Fig. 5*B*), a 76-kDa γ subunit species was predominantly observed in $\alpha\beta\gamma$-injected oocytes (*lane 4*). In the non-biotinylated protein pool (Fig. 5*C*), the 87-kDa full-length species was predominantly observed (*lanes 1–4*) with very little, if any, evidence of the 76-kDa species. However, this 76-kDa fragment was readily detected in the non-biotinylated membrane-enriched pool in all injection conditions along with the 87-kDa band (Fig. 5*D*, *lanes 1–4*). After a 24-h incubation (Fig. 5*A*), the γ_{mut} subunit expressed alone (*lane 5*) or γ_{mut} co-expressed with β (*lane 7*) did not generate any significant amiloride-sensitive current, whereas γ_{mut} co-expressed with α (*lane 6*) yielded around 5% of maximal activity observed when the $\alpha\beta\gamma_{mut}$ subunits were co-injected (*lane 8*). Importantly, the level of activity was identical to that of wild

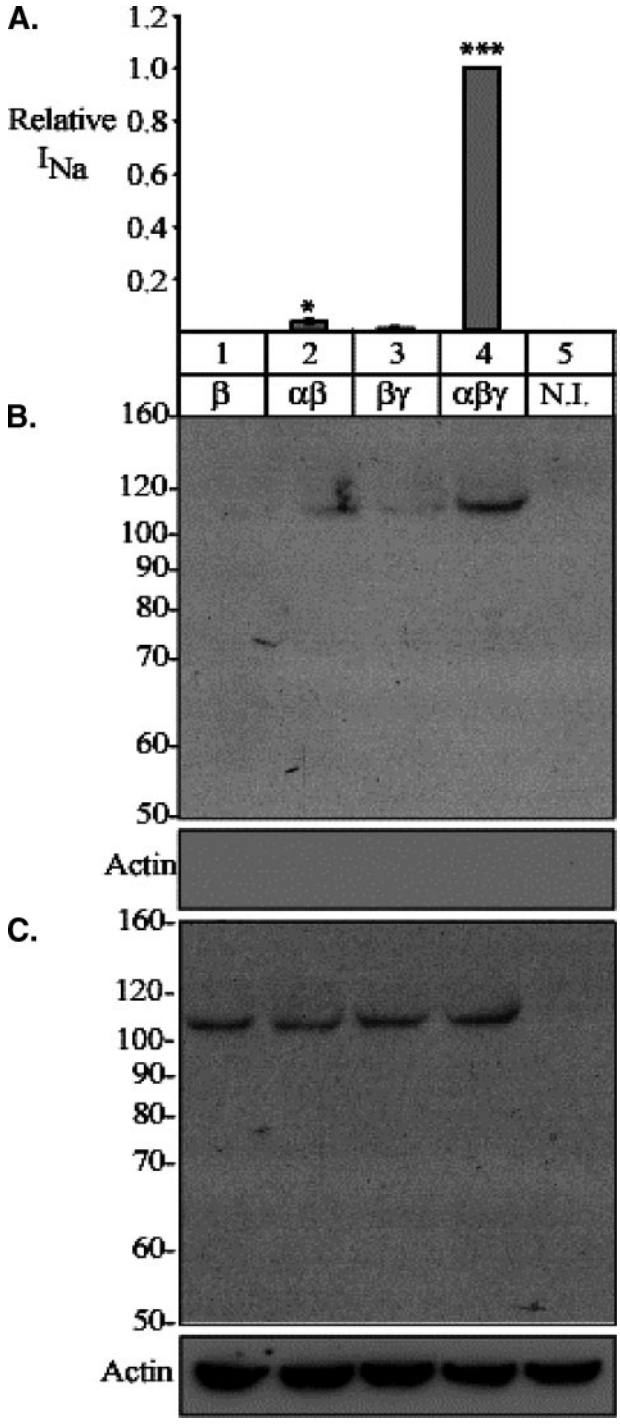

FIGURE 3. **Cell surface expression of β rENaC when assembled with α rENaC and/or γ rENaC.** *Xenopus* oocytes were injected with β, αβ, βγ, or αβγ rENaC cRNAs 24 h before experimental analysis. The β rENaC subunit was V5-tagged at the C terminus. Cell surface-biotinylated proteins and non-biotinylated proteins were probed with V5 antibody to detect the V5 tag inserted in the C terminus of β ENaC. *A*, amiloride-sensitive current. Current was measured by voltage clamp in each experimental condition and expressed relative to current in αβγ rENaC-injected oocytes (477 ± 166 nA; $n = 3$ independent experiments). Oocytes injected with αβγ rENaC had a significantly higher amiloride-sensitive current than β, αβ, and βγ rENaC-injected oocytes (*, $p < 0.001$), and αβ had a significantly higher amiloride-sensitive current than β rENaC-injected oocytes (***, $p < 0.05$). *B*, biotinylated cell surface proteins. Full-length 105-kDa β ENaC was detected at the cell surface in αβγ rENaC-injected oocytes, corresponding with oocytes exhibiting high channel activity. *C*, non-biotinylated protein pool. The non-biotinylated protein pool contained full-length 105-kDa β ENaC. Absence of actin in the biotinylated proteins indicated that no intracellular proteins were labeled. Even quantities of actin in the non-biotinylated proteins indicated even protein loading. *N.I.*, non-injected oocytes.

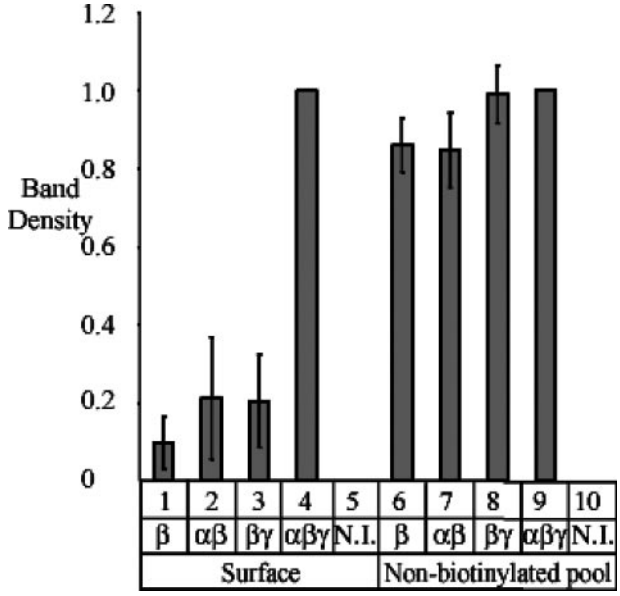

FIGURE 4. **Densitometry of β rENaC cell surface expression when assembled with α rENaC and/or γ rENaC.** Western blots of biotinylated and non-biotinylated protein in *Xenopus* oocytes injected with V5-tagged β rENaC alone and with α rENaC and/or γ rENaC were subjected to densitometric analysis ($n = 3$). Oocytes injected with αβγ rENaC had significantly more 105-kDa bands at the cell surface than β, αβ, and βγ rENaC-injected oocytes ($p < 0.001$). No significant difference was detected between the experimental groups in the 105-kDa band in the non-biotinylated protein pool. *N.I.*, non-injected oocytes.

type channels (Fig. 5*A*, *lane 4 versus lane 8*). At the cell surface (Fig. 5*B*), only the full-length 87-kDa species was observed, whereas the 76-kDa γ subunit species was conspicuously absent in $\alpha\beta\gamma_{mut}$-injected oocytes, indicating that the furin consensus site was no longer used by endogenous furin or furin-like proteases. In the non-biotinylated protein pool (Fig. 5*C*), only the 87-kDa full-length species was observed (*lanes 5–8*), with no evidence of the 76-kDa species even after long-term exposure (data not shown). In the non-biotinylated membrane-enriched protein pool (Fig. 5*D*), there was no evidence of the 76-kDa fragment, a fragment that was clearly identified in wild type channel complexes (*lanes 1–4 versus lanes 5–8*).

Quantitation of six independent γ assembly experiments is shown in Fig. 6. Upon preferential assembly of αβγ complexes, there was a large variation in cell surface expression of the full-length 87-kDa γ subunit (Fig. 6*A*, *lanes 1–4*). There was a >10-fold increase ($p < 0.001$) in the expression of the cleaved 76-kDa species in fully assembled αβγ channels (Fig. 6*A*, *lane 8*) compared with αγ (*lane 6*) or βγ (*lane 7*) complexes. This increase correlated with a 4-fold decrease ($p < 0.05$) of the 87-kDa species in the non-biotinylated total protein pool (Fig. 6*B*), but not in the non-biotinylated membrane pool (*panel C*). There was a correlation between γ cleavage and I_{Na}, suggesting a causal relationship. To test this hypothesis, we performed experiments with γ_{mut}.

γ_{mut} Subunit—If cleavage of γ by furin is essential for channel activation, it is expected that prevention of furin-specific cleavage should prevent ENaC activation. Upon preferential assem-

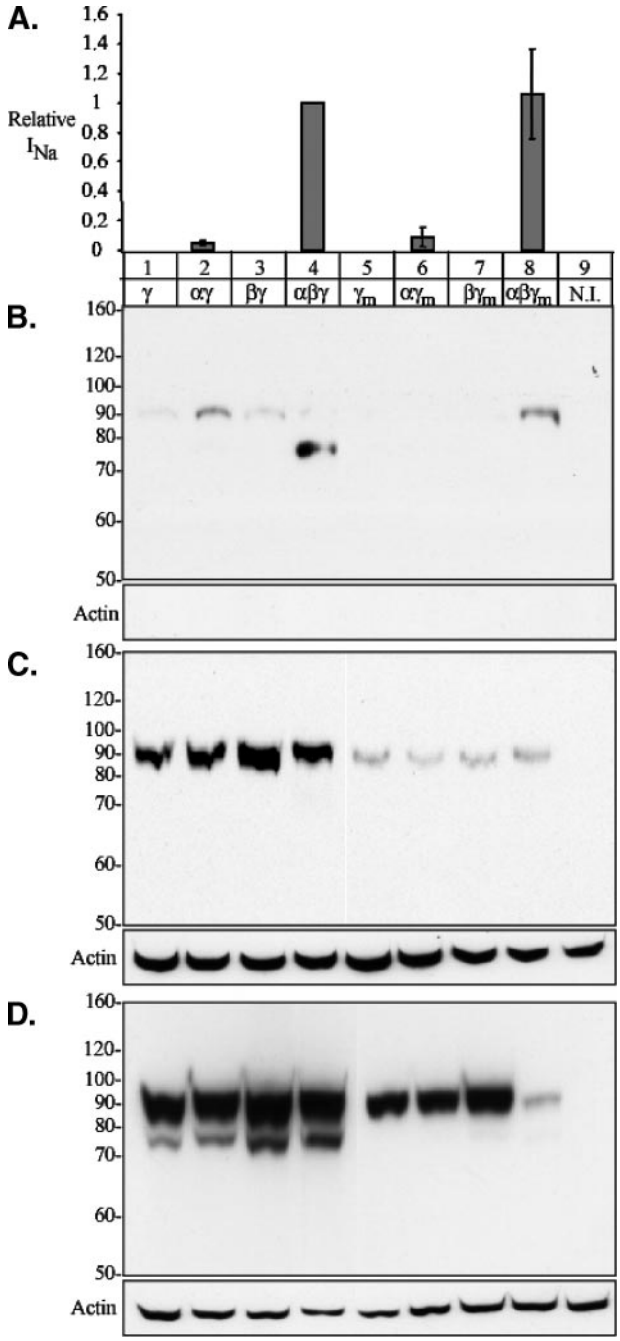

FIGURE 5. **Activity and expression of γ rENaC when assembled with α rENaC and/or β rENaC with and without mutations in the γ subunit furin cleavage site.** *Xenopus* oocytes were injected with γ, αγ, βγ, or αβγ rENaC cRNAs with and without mutations in the furin consensus site in the γ subunit 24 h before experimental analysis. The γ rENaC subunit was V5-tagged at the C terminus. Cell surface-biotinylated proteins, non-biotinylated proteins, and membrane-enriched protein fractions were probed with V5 antibody to detect the V5 tag inserted in the C terminus of γ ENaC. *A*, amiloride-sensitive current. Current was measured by voltage clamp in each experimental condition and expressed relative to current in αβγ rENaC-injected oocytes (2389 ± 406 nA; $n = 6$ independent experiments for WT, and $n = 3$ for experiments with the γ furin site mutation γ_{mut} ΔR138A). Oocytes injected with αβγ rENaC had a significantly higher amiloride-sensitive current than γ, αγ, and βγ rENaC-injected oocytes ($p < 0.001$), and αγ had a significantly higher amiloride-sensitive current than γ rENaC-injected oocytes ($p < 0.05$). Oocytes injected with $\alpha\beta\gamma_{mut}$ had currents not statistically different from αβγ-injected oocytes but higher than γ_{mut}-injected oocytes ($p < 0.001$). *B*, biotinylated cell surface proteins. Full-length 87-kDa γ ENaC was detected at the cell surface in the αγ rENaC injection condition, correlating with 5% channel activity. The 76-kDa γ ENaC cleavage product was only detected in the αβγ rENaC-injected condition, correlating with 100% channel activity. The 76-kDa cleaved band was not present at the surface of any of the oocytes injected with the γ_{mut} subunit. The 87-kDa band was present in the $\alpha\beta\gamma_{mut}$ injection condition only. *C*, non-biotinylated protein pool. The non-biotinylated protein pool contained predominantly full-length 87-kDa γ ENaC in all conditions; there were traces of the 76-kDa band in αβγ-injected oocytes, but not in $\alpha\beta\gamma_{mut}$-injected oocytes. *D*, membrane-enriched proteins. Membrane-enriched protein pellets contained full-length 87-kD γ ENaC as well as the 76-kDa cleavage product in each experimental condition with wild type γ rENaC. Only the 87-kDa uncleaved band was present in oocytes injected with the γ_{mut} subunit. The absence of actin in the biotinylated proteins indicated that no intracellular proteins were labeled. Even quantities of actin in the non-biotinylated and membrane-enriched proteins indicated even protein loading. *N.I.*, non-injected oocytes.

bly of $\alpha\beta\gamma_{mut}$ complexes (Fig. 6*A*, *lane 12*), there was a 3-fold decrease ($p < 0.05$) in cell surface expression of the full-length 87-kDa γ subunit compared with αβγ-injected oocytes (*lane 4*). Despite this relative decrease in cell surface expression, I_{Na} was identical to that of wild type channels (Fig. 5*A*, *lane 4 versus lane 8*), indicating that activation can occur independently of furin-dependent γ cleavage. There was a significant decrease of the 87-kDa species in the non-biotinylated protein pool (Fig. 5*B*, *lanes 9–12*). The non-biotinylated membrane pool (Fig. 5*C*) was less depleted compared with controls (*lanes 9–11 versus lanes 1–3*). By contrast, a very significant 90% decrease of the 87-kDa species was observed in the membrane fraction (Fig. 5*C*, *lane 12 versus lane 4*) These data suggest that the γ furin site mutation may interfere with protein synthesis and/or degradation. Despite that effect, ENaC activity measured as I_{Na} remained unchanged. We conclude that there is no causal relationship between γ cleavage and ENaC activation upon preferential assembly.

DISCUSSION

Furin-dependent and Furin-independent Mechanisms—The main findings of this study are 2-fold. First, assembly of the α, β, and γ ENaC subunits as functional (conducting) αβγ, αβ, and αγ heteromeric complexes greatly promotes surface expression of cleaved products of both the α and γ subunits. The endogenous proteases that cleave the α and γ subunits are not known with certainty. However, the leading candidates for major players are furin or furin-like enzymes. When the consensus sites for furin cleavage identified by Hughey *et al.* (10) were mutated, the 65-kDa α fragment and the 76-kDa γ fragment were no longer detected. Second, we discovered that specific elimination of furin-mediated cleavage had a range of effects on ENaC at the cell surface. Furin-mediated cleavage of the α subunit affected basal I_{Na}, whereas cleavage of the γ subunit affected overall expression levels. Although these observations are descriptive, we feel that they offer mechanistic insights into the roles of proteolysis in ENaC function.

Role of the 65-kDa α Fragment—Upon assembly of α into αβγ complexes, both the I_{Na} and intensity of the 65-kDa fragment increased (Figs. 1 and 2). When the α furin sites were mutated, the 65-kDa fragment disappeared, and base-line I_{Na} was reduced by 60% ($p < 0.01$). The cellular location where cleavage occurs was not identified by the present data, but it is clear that cleavage is promoted by channel assembly. The furin gene family encodes proprotein convertases that are expressed in various cellular compartments of the exocytic pathway.

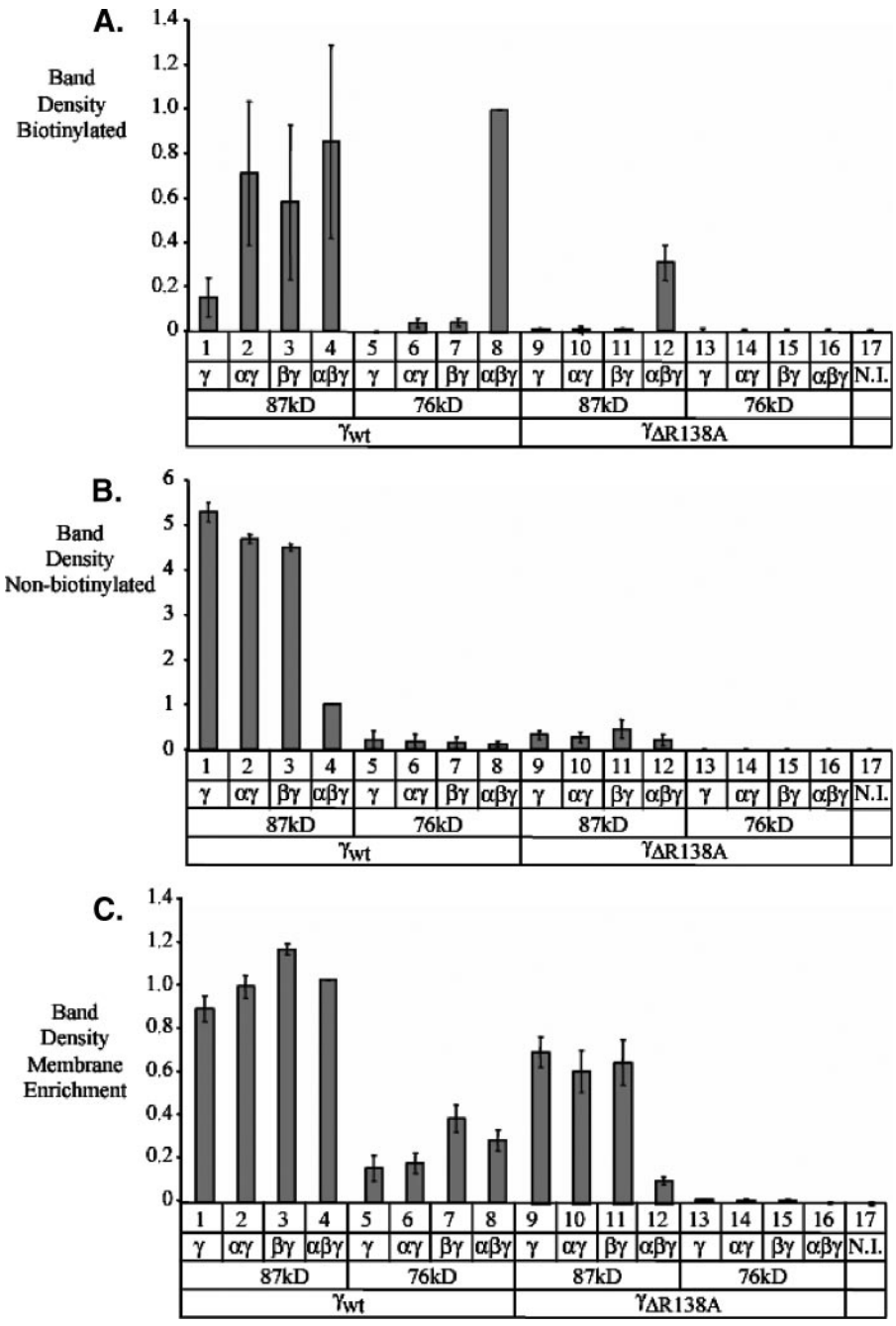

FIGURE 6. **Densitometry of γ rENaC cell surface expression when assembled with α rENaC and/or β rENaC with and without mutations in the γ subunit furin cleavage site.** Western blots of biotinylated, non-biotinylated, and membrane-enriched proteins from *Xenopus* oocytes injected with V5-tagged γ rENaC alone and with α rENaC and/or β rENaC with and without mutations in the γ subunit furin cleavage site were subjected to densitometric analysis. In biotinylated and non-biotinylated experiments, $n = 6$ independent experiments for WT, and $n = 3$ for experiments with the γ furin site mutation γ_{mut} ΔR138A. In membrane-enriched experiments, $n = 3$ for all conditions. *A*, cell surface biotinylation. Oocytes injected with $\alpha\beta\gamma$ rENaC had significantly more 76-kDa bands at the cell surface than γ rENaC-injected oocytes ($p < 0.001$). There was significantly less 87-kDa γ_{mut} ENaC at the cell surface in $\alpha\beta\gamma_{mut}$ ($p < 0.05$) than in $\alpha\beta\gamma$ controls. There were significantly fewer 76-kDa bands at the cell surface in $\alpha\beta\gamma_{mut}$-injected oocytes ($p < 0.001$). *B*, non-biotinylated proteins. There was significantly less full-length 87-kDa γ rENaC in $\alpha\beta\gamma$ rENaC-injected oocytes than in γ rENaC-injected oocytes in the non-biotinylated protein pool ($p < 0.05$). There were very low quantities of 76-kDa γ rENaC in the non-biotinylated protein pool, and no significant difference was detected between the experimental groups. There were significantly fewer 87-kDa bands in oocytes injected with γ_{mut}, $\alpha\gamma_{mut}$, $\beta\gamma_{mut}$, and $\alpha\beta\gamma_{mut}$ than with the wild type subunit ($p < 0.05$, 0.01, 0.05, and 0.01, respectively). *C*, membrane-enriched proteins. There was no difference in the quantity of 87- or 76-kDa bands in the wild type oocytes in the membrane-enriched proteins. There were significantly fewer 87-kDa bands in oocytes injected with $\alpha\gamma_{mut}$, $\beta\gamma_{mut}$, and $\alpha\beta\gamma_{mut}$ than the wild type subunit ($p < 0.05$, 0.01, and 0.001, respectively). There were significantly fewer 76-kDa bands in oocytes injected with $\alpha\gamma_{mut}$, $\beta\gamma_{mut}$, and $\alpha\beta\gamma_{mut}$ than the wild type subunit ($p < 0.05$, 0.01, and 0.001, respectively). *N.I.*, non-injected oocytes.

These proconvertases can activate their substrates in the endoplasmic reticulum and Golgi, as well as at the plasma membrane. The anthrax toxin receptor is a well described example of furin-mediated cleavage at the cell surface (see review in Ref. 13). We readily detected the 65-kDa fragment in the biotinylated pool, but not in the non-biotinylated pool, even when enriched for membrane proteins. In our work and as broadly recognized in other studies, only a small percentage of total ENaC is typically present at the cell surface. Thus, the α subunit is cleaved by an active enzyme at the plasma membrane or in a rapid turning-over membrane pool very near the plasma membrane. Kinetic experiments are needed to answer this question.

The disappearance of the 65-kDa fragment and decreased I_{Na} with α_{mut} suggest a causal relationship between α cleavage and partial ENaC activation. Interestingly, α_{mut} did not inhibit ENaC activation upon assembly of heteromeric $\alpha_{mut}\beta$ complexes but, if anything, enhanced I_{Na} above WT $\alpha\beta$, reaching 50% of $\alpha\beta\gamma$ maximal activation. We propose that the β subunit (which does not undergo any proteolytic cleavage) plays a significant role in ENaC activation and may contribute to furin-independent activation of ENaC. Moreover, these data further indicate that significant I_{Na} is possible in complexes containing the α subunit with furin sites disabled.

Role of the 76-kDa γ Fragment—We show here that the 76-kDa γ fragment is observed at the cell surface upon $\alpha\beta\gamma$ assembly. This observation parallels that of the 65-kDa α furin fragment and may relate to the co-chaperone effects that the ENaC subunits exert upon each other (discussed below). However, our results do indicate differences between the behaviors of the 76-kDa γ and 65-kDa α fragments that may reflect the complexity of interplay between the α, β, and γ subunits. For example, in contrast to the α fragment, the γ fragment

was readily detected in the non-biotinylated membrane-enriched fraction (compare Figs. 1 and 5). Although this observation does not provide a specific interpretation, it does suggest that the α and γ ENaC subunits are processed differently.

In a further contrast between furin-mediated cleavage of α and γ, the 76-kDa γ fragment was not required for full ENaC activation (Figs. 5 and 6). Although this result is somewhat at variance with Hughey *et al.* (10), who reported a significant (nearly 40%) inhibition of I_{Na}, both studies agree that furin-mediated cleavage of the γ subunit is less significant for basal I_{Na} than is furin-specific cleavage of α. The reason for the apparent discrepancy is not clear, but our experimental protocol differs notably from theirs. In their experiments, a direct correlation between the cleaved subunit and activation at the membrane was not studied because the 76-kDa γ fragment was identified by Western blotting of the total cell lysate and was not quantified. Our semi-quantitative approach permits the quantitation of relative changes that occur upon preferential assembly and correlation with I_{Na}. Importantly, we can correlate I_{Na} with the only biochemical pool relevant to function, *i.e.* the biotinylated surface-expressed pool. This approach demonstrated that although γ_{mut} did not reduce I_{Na}, there was a marked decrease in full-length subunits at the surface. Interestingly, mutation of the furin sites in the α subunit had no such effect on surface expression. Thus, we speculate that the furin site in γ ENaC plays an important, but not yet understood, role in overall ENaC biosynthesis and/or stability.

In summary, we propose that ENaC activation upon assembly from homomer to heteromultimer complexes involves furin-dependent and furin-independent mechanisms in a complex interplay of interactions between the α, β, and γ subunits. The relationship of γ cleavage to heteromeric complexes remains unclear. It is tempting to speculate that cleavage at the furin site is a necessary first step to set the channel in a conformation sensitive for a second cleavage either by other endogenous proteases (CAP1/prostasin, CAP2, and CAP3) or by exogenous serine proteases, such as trypsin and elastase. This second-hit hypothesis is supported by recent experimental evidence of such a mechanism (12, 14).

Physiological Relevance—Our observations highlight several significant issues regarding proteolytic regulation of ENaC. First, our study further defines and emphasizes the distinct and non-equivalent roles of individual subunits that have been previously noted, even from the initial cloning studies. Each subunit clearly undergoes a different extent of furin-mediated proteolysis, and the differences we observed in subcellular location of the 65-kDa α and 76-kDa γ fragments suggest that proteolysis at the "furin" sites may occur in different compartments. In addition, the participation of cleaved subunits in heteromeric complexes is already felt to influence critical channel characteristics, such as open probability, but other characteristics, such as dwell time at the cell surface, could be influenced. Second, we observed robust residual current of mutant channels that cannot be efficiently cleaved by furin or furin family members that share the same canonical R*XX*R cleavage sites. Our data do not allow us to choose among several interesting interpretations for this observation. For example, our data are formally consistent with the idea that cleavage by furin or furin-like enzymes is not required for channel activity. As the P1 arginine is a stringent requirement for furin and furin family members, this may turn out to be narrowly true. However, it is also likely that other proteases can act on ENaC subunits at other residues within the furin sequence or at nearby residues. More detailed mutagenesis and single channel studies may address these possibilities.

What is the *in vivo* physiological relevance of our findings? The cleavage of the γ subunit was first observed *in vivo* by Masilamani *et al.* (15). In their study, long-term salt deprivation of rats caused a 60-fold increase in plasma aldosterone and a shift in molecular mass of the γ ENaC subunit in the kidney that was consistent with a physiological proteolytic clipping of the extracellular loop. This finding was confirmed using a 15-h salt deprivation, causing a 2-fold increase in plasma aldosterone. Recently Ergonul *et al.* (16) were able to quantitate this effect under experimental maneuvers (sodium deprivation, potassium loading, aldosterone infusion, and resalination) that induce a large physiological range of plasma aldosterone concentrations. The authors concluded that changes in the processing and maturation of the channel involving the α and γ subunits occur rapidly enough to be involved in the daily regulation of ENaC activity and sodium reabsorption by the kidney (17). Of interest, the processing of the γ subunit measured in the total protein pool of kidney cortex *in vivo* is consistent with the changes we observed here upon channel assembly *in vitro*. It is known that *in vivo* aldosterone promotes rapid assembly and translocation of channel subunits from an intracellular vesicular pool to the apical pole and apical membrane of the connecting tubule and early collecting duct (18). The increased transcription/translation of the α subunit would rapidly favor its assembly with a pool of preformed β and γ subunits and promote their translocation to the apical pole or apical membrane of the aldosterone-sensitive distal nephron, which is composed of the late distal convoluted tubule, the connecting tubule, and the collecting duct. The critical role of the α subunit in this process is underscored by the lack of channel translocation in the collecting duct and by the normal translocation in the connecting tubule of mice genetically engineered to lack the α subunit of ENaC in the collecting duct but with ENaC expression in the connecting tubule left intact (19). Obviously, it will be technically challenging to identify the molecular species expressed *in vivo* in the apical membrane of aldosterone-sensitive distal nephron cells.

Acknowledgment—We thank Nicole Fowler Jaeger for technical help.

REFERENCES

1. Kellenberger, S., and Schild, L. (2002) *Physiol. Rev.* **82,** 735–767
2. Jasti, J., Furukawa, H., Gonzales, E. B., and Gouaux, E. (2007) *Nature* **449,** 316–323
3. Firsov, D., Gautschi, I., Merillat, A. M., Rossier, B. C., and Schild, L. (1998) *EMBO J.* **17,** 344–352
4. Snyder, P. M., Cheng, C., Prince, L. S., Rogers, J. C., and Welsh, M. J. (1998) *J. Biol. Chem.* **273,** 681–684
5. Eskandari, S., Snyder, P. M., Kreman, M., Zampighi, G. A., Welsh, M. J., and Wright, E. M. (1999) *J. Biol. Chem.* **274,** 27281–27286
6. Firsov, D., Gruender, S., Schild, L., and Rossier, B. C. (1997) *Nova Acta Leopoldina* **302,** 13–22

7. Firsov, D., Schild, L., Gautschi, I., Merillat, A. M., Schneeberger, E., and Rossier, B. C. (1996) *Proc. Natl. Acad. Sci. U. S. A.* **93,** 15370–15375
8. Bonny, O., Chraibi, A., Loffing, J., Jaeger, N. F., Grunder, S., Horisberger, J. D., and Rossier, B. C. (1999) *J. Clin. Investig.* **104,** 967–974
9. Hughey, R. P., Mueller, G. M., Bruns, J. B., Kinlough, C. L., Poland, P. A., Harkleroad, K. L., Carattino, M. D., and Kleyman, T. R. (2003) *J. Biol. Chem.* **278,** 37073–37082
10. Hughey, R. P., Bruns, J. B., Kinlough, C. L., Harkleroad, K. L., Tong, Q., Carattino, M. D., Johnson, J. P., Stockand, J. D., and Kleyman, T. R. (2004) *J. Biol. Chem.* **279,** 18111–18114
11. Michlig, S., Harris, M., Loffing, J., Rossier, B. C., and Firsov, D. (2005) *J. Biol. Chem.* **280,** 38264–38270
12. Harris, M., Firsov, D., Vuagniaux, G., Stutts, M. J., and Rossier, B. C. (2007) *J. Biol. Chem.* **282,** 58–64
13. Abrami, L., Reig, N., and van der Goot, F. G. (2005) *Trends Microbiol.* **13,** 72–78
14. Bruns, J. B., Carattino, M. D., Sheng, S., Maarouf, A. B., Weisz, O. A., Pilewski, J. M., Hughey, R. P., and Kleyman, T. R. (2007) *J. Biol. Chem.* **282,** 6153–6160
15. Masilamani, S., Kim, G. H., Mitchell, C., Wade, J. B., and Knepper, M. A. (1999) *J. Clin. Investig.* **104,** R19–R23
16. Ergonul, Z., Frindt, G., and Palmer, L. G. (2006) *Am. J. Physiol.* **291,** F683–F693
17. Frindt, G., McNair, T., Dahlmann, A., Jacobs-Palmer, E., and Palmer, L. G. (2002) *Am. J. Physiol.* **283,** F717–F726
18. Loffing, J., Zecevic, M., Feraille, E., Kaissling, B., Asher, C., Rossier, B. C., Firestone, G. L., Pearce, D., and Verrey, F. (2001) *Am. J. Physiol.* **280,** F675–F682
19. Rubera, I., Loffing, J., Palmer, L. G., Frindt, G., Fowler-Jaeger, N., Sauter, D., Carroll, T., McMahon, A., Hummler, E., and Rossier, B. C. (2003) *J. Clin. Investig.* **112,** 554–565